

Variable Hall coefficient in $\text{Bi}_2\text{Sr}_2\text{CaCu}_2\text{O}_{8-x}$ across the metal-insulator transition

G. Briceno and A. Zettl

Department of Physics, University of California at Berkeley,
and Materials and Chemical Sciences Division, Lawrence Berkeley Laboratory, Berkeley, California 94720
(Received 9 August 1989)

Measurements are reported of the Hall coefficient R_H and ab -plane resistivity for single-crystal $\text{Bi}_2\text{Sr}_2\text{CaCu}_2\text{O}_{8-x}$, with variable oxygen configuration. As the system is driven through the metal-“insulator” transition, R_H increases strongly but continues to obey the empirical expression $1/R_H = \gamma + \beta T$, where T is the temperature. For low oxygen content the Hall mobility μ_H becomes temperature independent. We examine these results in terms of various normal-state transport models.

In several new classes of Cu-O based superconducting oxides, the normal state is characterized by either hole or electron carriers in low concentration, with moderate to severe structural and electrical anisotropy. The transport properties are often very different from those expected for a simple metal, and are sensitive to chemical doping (in particular oxygen). Recently, it was demonstrated¹ that for $\text{Bi}_2\text{Sr}_2\text{CaCu}_2\text{O}_{8-x}$ a metal-“insulator” transition can be induced by changing the oxygen configuration (i.e., the actual oxygen content with possible associated defect structure). The term insulator here refers to a nonmetallic state where the electrical resistivity increases with decreasing temperature, similar to semiconducting behavior. Both the resistivity and thermoelectric power obey simple empirical expressions with application to other high- T_c oxides.^{1,2}

In this paper we report on experiments measuring simultaneously the ab -plane Hall coefficient R_H and ab -plane normal-state resistivity ρ_{ab} of $\text{Bi}_2\text{Sr}_2\text{CaCu}_2\text{O}_{8-x}$ single crystals. The temperature dependences of both R_H and ρ_{ab} follow simple functional forms, which remain intact as the sample is driven across the (loosely defined) metal-insulator transition by oxygen depletion. We use these transport coefficients to extract characteristic transport parameters, and compare our results to the predictions of various novel normal-state conduction mechanisms.

High-purity single crystals of $\text{Bi}_2\text{Sr}_2\text{CaCu}_2\text{O}_{8-x}$ were grown from a mixture of Bi_2O_3 , SrCO_3 , CaCO_3 , and CuO as described elsewhere.³ The crystals were cleaved and cut into thin ab -plane sheets of typical dimensions $2.0 \text{ mm} \times 1.0 \text{ mm} \times 10 \text{ } \mu\text{m}$, where the small dimension corresponds to the c -axis direction. The samples were optically smooth and shiny and had no major visible defects. The resistivity was measured using a modified linear four-probe contact configuration with fired-on silver paint contact pads, and the Hall voltage was obtained simultaneously using an ac current source and lock-in detection with a five-probe arrangement.⁴ The magnetic field was oriented parallel to the c axis, and hence the Lorentz force was in the ab plane. R_H showed linearity in applied current up to 1.0 mA and applied magnetic field up to 10 kG, the maximum values applied.

Figure 1 shows the ab -plane resistivity and Hall

coefficient of a particular $\text{Bi}_2\text{Sr}_2\text{CaCu}_2\text{O}_{8-x}$ crystal for four different oxygen configurations. The lower half of the figure shows the temperature-dependent resistivity. Curve *A* is for the crystal following an initial high oxygen anneal (5 h at 650°C , followed by a 12-h ramp to 25°C , in 1-atm O_2 flow). The resistivity is linear and metallic

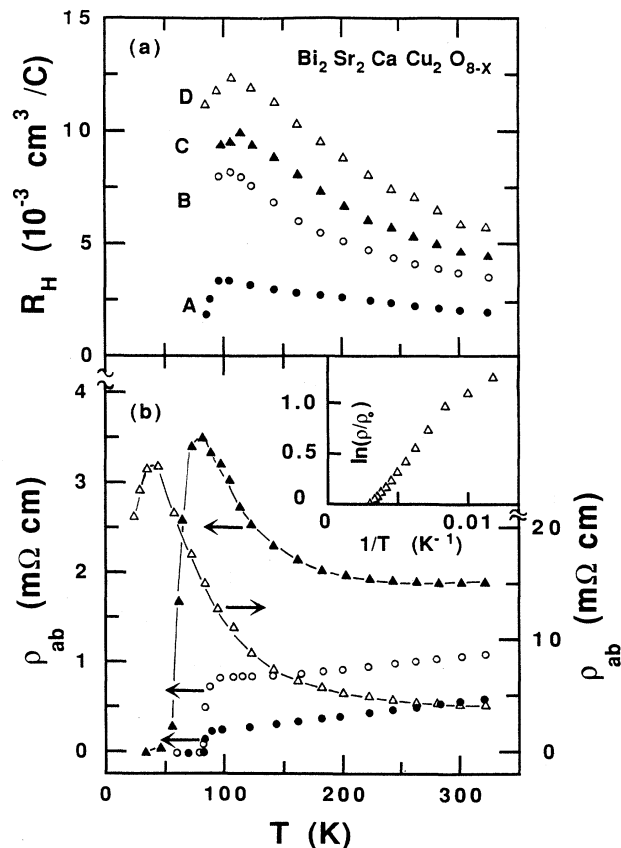


FIG. 1. Hall coefficient and resistivity for the ab plane of a $\text{Bi}_2\text{Sr}_2\text{CaCu}_2\text{O}_{8-x}$ single crystal for different oxygen configurations. Sample *A* has the highest oxygen content, while sample *D* has the lowest (see text). The inset shows the resistivity data of sample *D* replotted in a form where a straight line would indicate activated conduction (not observed).

before dropping to zero at $T_c \approx 83$ K. Curves *B-D* are for the same crystal with successively lower oxygen concentration. Consistent with previous work,¹ oxygen depletion changes ρ_{ab} from metalliclike to insulatorlike (or semiconductorlike), with a concomitant depression of T_c . The oxygen configuration of sample "B" was established through a low oxygen anneal cycle (5 h at 325°C, followed by a 12-h ramp to 25°C, all at ~ 10 mTorr O_2). This treatment increased the resistivity by a factor of 2, still showing metallic behavior (curve *B*) down to ~ 130 K, where it shows a small upturn before dropping to zero at $T_c \approx 81$ K. The same sample was subjected to another low oxygen anneal cycle (5 h at 345°C, followed by a 12-h ramp to 25°C, all at ~ 10 mTorr O_2), after which the resistivity (curve *C*) increased by a factor of 3 from the original high oxygen concentration state at room temperature. Here the semiconductive upturn begins at ~ 250 K and continues down to $T_c \approx 62$ K. Once again, the sample was subjected to another low oxygen anneal cycle (5 h at 375°C, followed by a 12-h ramp to 25°C, all at ~ 10 mTorr O_2), after which the resistivity (curve *D*) showed a total increase by an order of magnitude, with semiconductorlike behavior observed between room temperature and $T_c \approx 25$ K. The inset to Fig. 1(b) shows the resistivity data of curve *D* replotted as $\ln\rho/\rho_0$ vs $1/T$, where ρ_0 is the room-temperature resistivity. Simply activated behavior is not observed, hence the resistivity differs quantitatively from true semiconducting behavior.

Figure 1(a) shows the Hall coefficient (measured simultaneously with the resistivity), following the successive anneal cycles described above. The symbols correspond to those of the resistivity specimens [Fig. 1(b)]. For all oxygen configurations, the Hall coefficient grows as the temperature is decreased, down to about 100 K, below which superconducting fluctuation effects dominate. At fixed temperature, the general trend is that a decreased oxygen content increases the Hall coefficient. R_H shows an increase by a factor of 2.9 from the high oxygen anneal cycle (curve *A*) to the extreme low oxygen anneal cycle (curve *D*) at room temperature. Using the expression $R_H = 1/nec$, we find at room temperature an effective hole concentration $n = 3.02 \times 10^{21} \text{ cm}^{-3}$ for the high oxygen specimen (curve *A*), and $n = 1.05 \times 10^{21} \text{ cm}^{-3}$ for the low oxygen specimen (curve *D*). Normalized to the unit-cell volume ($3.813 \times 3.813 \times 30.67 \text{ \AA}^3$), this corresponds to $n_H = 1.36$ and 0.474 holes per unit cell, for the high and low oxygen specimens, respectively.

The dramatic difference in the *ab*-plane resistivity and Hall coefficient observed in Fig. 1 for the different specimens of $\text{Bi}_2\text{Sr}_2\text{CaCu}_2\text{O}_{8-x}$ is directly related to oxygen configuration. Although we are not able to nondestructively determine the actual oxygen content of the different specimens within a resolution greater than $x = 0 \pm 0.1$ (using weight loss and Rutherford backscattering), from previous studies⁵ we estimate a value of $x \approx 0.08$ after the extreme low oxygen anneal cycle. Structural single-crystal x-ray studies on similar crystals showed the presence of stacking faults, but no secondary phases (independent of the oxygen configuration).

Previous Hall-effect measurements in $\text{YBa}_2\text{Cu}_3\text{O}_{7-\delta}$ (Refs. 6 and 7) suggest a Hall number ($\sim 1/R_H$) propor-

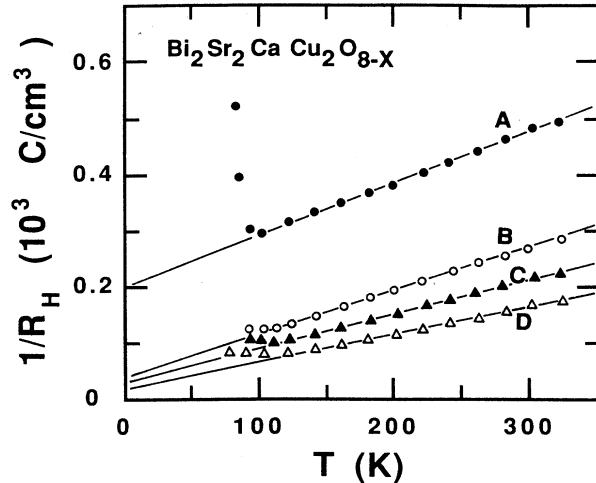


FIG. 2. $1/R_H$ for the *ab* plane of $\text{Bi}_2\text{Sr}_2\text{CaCu}_2\text{O}_{8-x}$ showing good agreement with Eq. (1) above T_c for different oxygen configurations (*A* has the highest oxygen content, while *D* has the lowest; see text). The $1/R_H$ data can be converted to Hall number n_H (holes per unit cell) by multiplying by $2.78 \times 10^{-3} \text{ cm}^3/\text{C}$.

tional to temperature T . A similar relation has been suggested for Bi-Sr-Ca-Cu-O and $\text{Tl}_2\text{Ca}_2\text{Ba}_2\text{Cu}_3\text{O}_x$ ceramics.⁸ Figure 2 shows the inverse Hall coefficient $1/R_H$ plotted versus T for the four different oxygen configurations. The plot indicates, for all four specimens, good agreement with the expression

$$1/R_H = \gamma + \beta T, \quad (1)$$

where γ and β are constants. As the oxygen deficiency is increased, the zero-temperature offset γ is reduced from $0.2 \times 10^3 \text{ C/cm}^3$ toward zero, and the slope β decreases from 0.920 to 0.480 $\text{C/cm}^3\text{K}$.

Figure 3 shows the Hall mobility μ_H extracted from the Hall coefficient and *ab*-plane resistivity measurement for

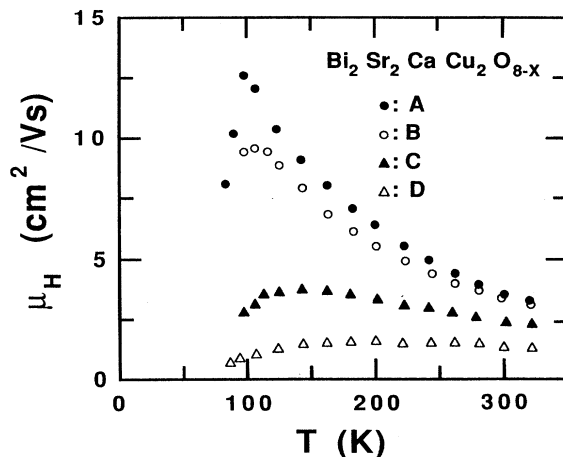


FIG. 3. Hall mobility for the *ab* plane of $\text{Bi}_2\text{Sr}_2\text{CaCu}_2\text{O}_{8-x}$ crystals for different oxygen configurations (*A* has highest oxygen content, while *D* has lowest; see text).

the four different oxygen configurations. We see that the Hall mobility decreases as oxygen is depleted from the sample and the specimen becomes more insulating. For high oxygen (metallic) samples (curves *A* and *B*) the mobility is very temperature dependent (behaving roughly as $1/T$), while for low oxygen content (curve *D*) μ_H appears to saturate and becomes roughly temperature independent.

The resistivity and Hall data of Fig. 1, and Eq. (1) in particular, are not generally consistent with simple metallic (band) behavior. Nevertheless, we briefly examine the consequences of a simple metallic transport model which allows evaluation of characteristic fundamental parameters. The temperature-dependent resistivity $\rho_{e-ph}(T) = m^*/ne^2\tau_{e-ph}(T)$ relates the carrier concentration n and scattering time τ_{e-ph} . At sufficiently high temperature, τ_{e-ph} varies inversely with T and is related to the transport electron-phonon coupling parameter λ_{tr} by $\hbar/2\pi\tau_{e-ph} = 2\pi\lambda_{tr}k_B T$. λ_{tr} is a good estimate of λ which determines T_c in Eliashberg theory. The most metallic sample (curve *A*) in Fig. 1 has a resistivity slope $1.46 \mu\Omega \text{ cm/K}$. Combining this with the room temperature $n = 3.02 \times 10^{21} \text{ cm}^{-3}$, we estimate $\tau_{e-ph} = 0.62 \times 10^{-12} (m^*/m) T^{-1}$ (sec K) and $\lambda_{tr} = 1.95 (m/m^*)$ for the high oxygen specimen. Within conventional BCS electron-phonon superconductor theory, an electron-phonon coupling parameter of this order is not unreasonable for the observed T_c of 85 K.

Numerous other transport models have been suggested for the high- T_c oxides. Two-band models^{9,10} are problematical in that the observed temperature dependence of R_H restricts too severely the band parameters,¹¹ and in a way inconsistent with pressure studies¹² (at least for $\text{YBa}_2\text{Cu}_3\text{O}_7$). Strong electron-electron interaction effects can lead to the opening of a soft Coulomb gap at E_F ,^{13,14} with a resulting resistivity $\rho \sim \exp(T_0/T)^{1/2}$. In two dimensions, additional disorder leads¹⁵ to a scaling between the fractional increase in ρ and the fractional increase in R_H : $\delta R_H/R_H = 2\delta\rho/\rho$. At relatively low temperatures, curves *C* and *D* in Fig. 1(b) roughly follow such an exponential temperature dependence, but we fail to find a scaling with R_H . Hence, we rule out the Coulomb-gap behavior in this parameter range of $\text{Bi}_2\text{Sr}_2\text{CaCu}_2\text{O}_{8-x}$.

Another model, used previously¹⁶ to interpret resistivity and Hall data for insulating La_2CuO_4 , is that of a doped semiconductor. However, the conductivity and Hall coefficient for this process are both simply activated, in contrast to our findings for $\text{Bi}_2\text{Sr}_2\text{CaCu}_2\text{O}_{8-x}$ here. We also note that the thermoelectric power of $\text{Bi}_2\text{Sr}_2\text{CaCu}_2\text{O}_{8-x}$ was shown previously¹ to obey the expression $S = A + BT$, with A and B constants (A depends on oxygen configuration). This expression is also obtained for small polaron hopping transport, and has been applied to the boron carbides.¹⁷ However, the predicted Hall coefficient for polaron hopping is not consistent with Eq. (1) and the data for Fig. 1(a).

We have previously demonstrated that in $\text{Bi}_2\text{Sr}_2\text{CaCu}_2\text{O}_{8-x}$ (Ref. 1) and $\text{YBa}_2\text{Cu}_3\text{O}_{7-\delta}$ (Ref. 18) the resistivity closely follows the empirical expression

$$\rho(T) = \rho_0 T^a \exp(\Delta/k_B T), \quad (2)$$

where a is between 0.5 and 1.0. Combining Eqs. (1) and (2) yields a mobility consistent with Fig. 3. The physical justification of Eq. (2) is not clear, but it may arise from a quantum-percolation-type transport as suggested by Phillips.¹⁹

In conclusion, the resistivity and the Hall constant of $\text{Bi}_2\text{Sr}_2\text{CaCu}_2\text{O}_{8-x}$ are extremely sensitive to oxygen configuration. The temperature dependence of these transport coefficients follows simple empirical expressions. The Hall constant for the magnetic field applied perpendicular to the Cu-O planes is p type with a $1/T$ behavior for different oxygen configurations. This unusual behavior has also been observed in other high- T_c oxides suggesting that these expressions may be inherent to the high- T_c superconductors.

The authors wish to acknowledge the useful conversations with Amy Y. Liu and Marvin L. Cohen. This research was supported in part by the Director, Office of Energy Research, Office of Basic Energy Sciences, Materials Sciences Division of the U.S. Department of Energy under Contract No. DE-AC03-76SF00098. Additional support was received from National Science Foundation Grant No. DMR 84-00041.

¹M. C. Crommie, Amy Y. Liu, Marvin L. Cohen, and A. Zettl (unpublished).
²M. C. Crommie, G. Briceno, and A. Zettl, in Proceedings of the Materials and Mechanisms of High Temperature Superconductivity Conference, Stanford, California, 1989 (unpublished).
³J.-M. Imer *et al.*, Phys. Rev. Lett. **62**, 336 (1989).
⁴R. H. Friend and N. Bett, J. Phys. E **13**, 294 (1980).
⁵J. M. Tarascon *et al.*, Phys. Rev. B **37**, 9382 (1988); *ibid.* **38**, 8885 (1988).
⁶T. Penney, S. von Molnar, D. Kaiser, F. Holtzberg, and A. W. Kleinsasser, Phys. Rev. B **38**, 2918 (1988).
⁷Y. Iye, T. Tamegai, T. Sakakibara, T. Goto, N. Miura, H. Takeya, and H. Takei, Physica C **153+155**, 26 (1988).
⁸J. Clayhold, N. P. Ong, P. H. Hor, and C. W. Chu, Phys. Rev. B **38**, 7016 (1988).
⁹Y. Lu, Y. F. Yan, H. M. Duan, L. Lu, and L. Li (unpublished).

¹⁰D. M. Eagles, Physica C **153+155**, 701 (1988).
¹¹M. W. Shafer, T. Penney, and B. L. Olson, in *Novel Superconductivity*, edited by S. A. Wolf and V. Z. Kresin (Plenum, New York, 1987), p. 771.
¹²I. D. Parker and R. H. Friend, J. Phys. C **21**, L345 (1988).
¹³A. L. Efros and B. I. Shklovskii, J. Phys. C **8**, L49 (1975).
¹⁴P. Bernstein, J. Bok, and A. Zylbersztein, Solid State Commun. **70**, 271 (1989).
¹⁵B. L. Altshuler, D. Khmel'nitzkii, A. J. Larkin, and P. A. Lee, Phys. Rev. B **22**, 5142 (1980).
¹⁶N. W. Preyer, R. J. Birgeneau, C. Y. Chen, D. R. Gabbe, H. P. Janssen, M. A. Kastner, P. J. Picone, and Tineke Thio (unpublished).
¹⁷C. Wood and D. Emin, Phys. Rev. B **29**, 4582 (1984).
¹⁸M. C. Crommie *et al.*, Phys. Rev. B **39**, 4231 (1989).
¹⁹J. C. Phillips, *Physics of High- T_c Superconductors* (Academic, Boston, 1989).